

Escalating wildfires in Siberia driven by multiple climate feedbacks under a warming Arctic

Xin Huang^{1,2}, Lian Xue^{1,2}, Aijun Ding^{1,2}

¹School of Atmospheric Sciences, Nanjing University, Nanjing, 210023, China

²Frontiers Science Center for Critical Earth Material Cycling, Nanjing University, Nanjing, 210023, China

Abstract

Wildfire in Siberia is of paramount importance in the carbon cycle and climate change as it is a major disturbance in the pan-Arctic ecosystems. In recent decades, the Siberian wildfire regime has been changing; however, less is known about the key climatic drivers and the underlying feedback over these vulnerable fire-prone landscapes. Here, based on ground-based and satellite observations and meteorological reanalysis data during the past two decades (2002–2021), we find that central Siberia features the most prominent wildfire escalation and poleward expansion. Such a shift in wildfires is closely related to drying soil moisture under a fast-warming Arctic. Our results show that a warming air temperature and weakened meridional moisture flux substantially suppress precipitation and are responsible for an increasing hydrological drought in central Siberia. We also reveal an unexpected self-amplifying feedback induced by

smoke aerosol via modifying cloud microphysical properties, which further compounds wildfires in Siberia. As the Arctic warming is projected to continue, wildfires in this region are estimated to be intensified by 200–350% by the end of this century. This work identifies main climate drivers and feedback mechanism for the escalating wild-fire risk in Siberia since the onset of this century, highlighting the importance of risk management and fire-climate adaptation in this region.

Main

Boreal and Arctic terrestrial ecosystems have been serving as a carbon sink and are critically important in the global climate system^{1,2}. Arctic permafrost, storing nearly 1,700 billion metric tons of frozen and thawing carbon, is one of the world's largest carbon reservoirs. It is estimated that permafrost carbon reservoirs approximately double the global atmospheric carbon^{3,4}. However, pan-Arctic wildfires, including peatland and forest burning, would shift Arctic and boreal lands from carbon sinks to carbon sources via direct combustion emission as well as disrupting vegetation regeneration⁵⁻⁸. Furthermore, recent study demonstrated that wildfires are also intricately linked with permafrost degradation because the combustion of vegetation and soil carbon would warm permafrost and increase microbial respiration that even releases ancient carbon (>10,000 years old) into the atmosphere⁹. Across the pan-Arctic area, Siberian wildfire occurrence and severity has been predicted to increase in the upcoming decades with severe negative impacts¹⁰.

Ever-increasing carbon emissions from both biomass burning and fossil fuel combustion have been compounding the global warming. Across the globe, the Arctic warming is emerging as a scientific and societal concern because the warming trend in this region is found to be 2–4 times faster than that of the rest of the world over the past 30 years (also known as Arctic amplification)^{11,12}. It is worth noting that wildfires, especially extreme ones, are highly sensitive to climatic conditions, which are dominant large-

scale drivers of shaping the fire-prone landscapes and determining the fire weather condition^{13,14}. The warming trend of climate has been found to exacerbate wildfires via rising air temperature, deepening drought and suppressing precipitation, thereby making vegetation greatly combustible and driving rapid fire spread^{15,16}. In comparison with biomass burning in other regions, Siberian wildfires are exceptionally vulnerable to climate warming and its intensification is far more severe because the carbon-rich soil could get highly flammable as high air temperature thaw and dry the permafrost^{17,18}. In recent years, gigantic wildfires have been raging across Siberia on a record scale, which is getting increasingly severe and have sparked global concerns^{19,20}. An obvious increase in fire severity and lengthening of fire season since the beginning of the century has been detected in Siberia, which have been linked to the soaring air temperature. In 2020 when air temperatures north of the Arctic Circle hit a new record high, Arctic wildfires increased by 35% from the previous year and caused record-breaking emissions from 66 Mt to 143 Mt carbon released into the atmosphere²¹. Noteworthy, central and eastern Siberia have been found to show most significant increasing trend in trends with a positive air temperature trend²².

More than merely being responsive to climate, wildfire in turn influences climate by releasing heat-trapping greenhouse gas into the atmosphere²³, plausibly contributing to positive carbon-climate feedback. Even worse, wildfire smoke that contains a large amount of light-absorbing carbonaceous aerosols, including black carbon and organic

aerosol²⁴, has been demonstrated to substantially influence humidity conditions, atmospheric stability, and precipitation, in some cases giving rise to a positive fire-smoke-weather feedback^{25,26}. In the high latitudes, the climatic feedback of wildfire smoke is particularly complex. Fire-emitted carbonaceous aerosols not only perturb the radiation balance²⁷, but also modify cloud properties and deposit on the glacier surface²⁸, leading to a longer dry season and providing greater opportunities and frequency for extremely large fires. Thus, the complex feedbacks and interactions between fire and climate are big challenges that we face in understanding and managing wildfires.

Multiple lines of evidence have indicated that Siberian wildfire is greatly modulated by climate and is currently intensifying under a fast-warming Arctic^{17,29,30}. However, the climatic drivers, underlying feedbacks/interactions ongoing in the Arctic and future fire risk still need to be thoroughly explored and comprehensively assessed. Here, by integrating 20-year wildfire observation, meteorological reanalysis data together with climate-chemistry coupled modeling, we explore the primary driving forces of the escalating Siberian wildfire and its linkage with a fast-warming Arctic. On the basis of mechanism understanding, the fire risk in Siberia at the end of this century is assessed according to climate projection under typical shared socioeconomic pathways (SSP) within the Coupled Model Intercomparison Project Phases 6 (CMIP6).

Climate warming and poleward expansion of Siberian wildfire

Periodic wildfires are a permanent natural process of Siberian coniferous forests mainly consisting of larch, spruce, and pine, most of which are underlain by vast deposits of carbon-rich soil (Extended Data Figs. 1 and 2). Different from other biomass-burning regions, Siberian wildfires not only burn the surface vegetation, but also consume the organic soil, feeding large-size and long-duration fires with an enormous amount of fuel³¹. High-latitude wildfires, especially those above the Arctic Circle (north of 67°N), predominately concentrates to the east of Ural Mountains and to the west of Verkhoyansk Ranges (55–70°N, 60–140°E, hereafter called central Siberia, black rectangle in Fig. 1a and Extended Data Fig. 2). In the past 20 years, wildfire activities in central Siberia have more than doubled according to satellite-derived burned area estimation from both Moderate Resolution Imaging Spectroradiometer (MODIS) MCD64A1 Burned Area data product and Fire Inventory from National Center for Atmospheric Research (FINN) burned area estimation (Extended Data Fig. 3). The zonal-aggregated burned area of wildfire has increased from less than 40,000 km² in the early 2000s to ~80,000 km² in 2020s (Fig. 1c), corresponding to the recent findings that Siberian wildfires are getting clustered and intensified^{22,32}. In spatial, the region with most prominent wildfire escalation features a substantial warming tendency in the past two decades, especially area north of 60°N (Fig. 1a).

Such a drastic enhancement in wildfire activities in central Siberia is also well demonstrated by fire carbon emission. Quantitatively, the carbon emission estimation in central Siberia (black rectangle in Fig. 1a) derived from Global Fire Emissions Database

(GFED) soared from 22.9 Mt Carbon in 2000 to 351.5 Mt Carbon in 2020²⁴ (Extended Data Fig. 3). Besides from doubled burned area of wildfire in central Siberia, such a dramatic increase in carbon emission is also attributed to the spatial redistribution of wildfire activities. Satellite fire detection clearly demonstrates that the Siberian fire regimes have undergone substantial shifts. As illustrated in Fig. 1b and Extended Data Fig. 2, wildfires in central Siberia have been expanding northward and poleward in the past two decades. At the beginning of the 21st Century, large fires (zonal aggregated burned area greater than 100 km²) in central Siberia mostly occurred around 67°N and farther south, and hardly can any large fires scorch north of 70°N. However, wildfires have readily engulfed north of 71°N almost every single year since 2016, leading to unprecedented wildfires in the Arctic Circle. Smoke from wildfires raging in Siberia has even reached the North Pole in historic first in August 2021 (Extended Data Fig. 4). Such a poleward wildfire expansion would expose an increasing permafrost and the associated huge carbon reservoir to ravaging wildfires (Fig. 1b). By combining FINN burned area dataset and permafrost distribution derived from the European Space Agency's Climate Change Initiative Permafrost project (ESACCI, version 3)³³, it is estimated that the area of permafrost subjective to wildfires has increased by 75% in the past decade. Quantitatively, the area of permafrost exposed to wildfire in central Siberia during 2002–2011 was 161,472 km², while the corresponding value for 2012–2021 was as high as 282,213 km², further unlocking the huge soil carbon.

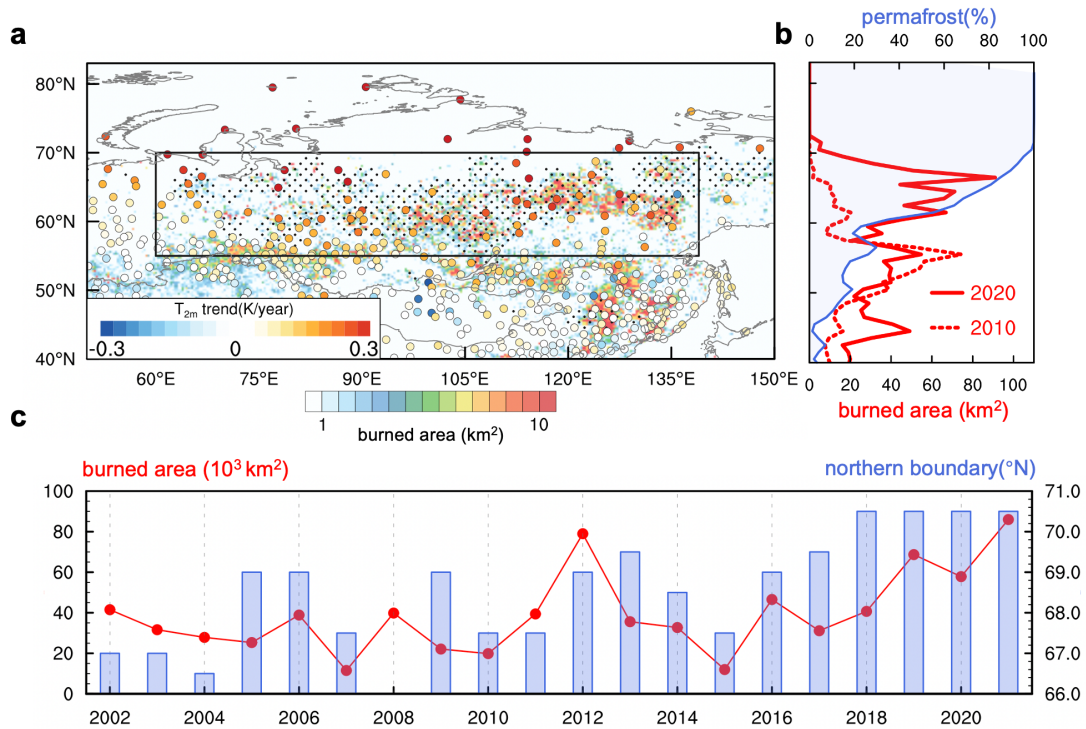


Fig 1. Siberian wildfire and warming trend in the past two decades. **a**, Map showing FINN burned area of wildfires and observed 2-meter air temperature trend during 2002–2021. The black dots mark the locations where the burned area have more than doubled in the past two decades. The black rectangle marks the study domain of this work. **b**, Zonal averaged (60–140 °E) permafrost coverage and wildfire burned area in 2010 and 2020. **c**, Northern boundary of large fires (zonal aggregated burned area greater than 100 km²) and burned area of wildfires in central Siberia (black rectangle in **a**) from 2002 to 2021.

Warming-induced drought as a key driver of the wildfire enhancement

As one of the most fire-prone landscapes with a large area of coniferous forests, seasonally, Siberia is generally subjected to intense wildfires from April to October as surface temperature gets warm and the snow line retreats²⁰. Generally, summer (June–August) features most vigorous wildfire activities in this region (Fig. 2a), and it also marks the season with the most significant expansion and intensification of Siberian wildfires (Extended Data Fig. 5). In this region, climatic conditions, like air temperature

and precipitation, have long been attributed as primary drivers modulating the interannual variability of wildfire frequency and intensity^{34,35}. To identify the key factors modulating central Siberian wildfires, we collected multiple meteorological parameters from the atmospheric reanalysis data (ERA5) during 2002–2021, including air temperature, relative humidity, wind, soil moisture, rainfall rate etc. Fig. 2a indicates that soil moisture dominates the interannual variations of central Siberia wildfire in summer and autumn. It coincides with the finding that warmer histosols with higher moisture deficiency are the most important factors creating and accelerating the ignition and spread of fires in this region^{18,36}.

During the summertime when the wildfires in central Siberia show the fastest poleward intensification, the correlation coefficient of fire area on soil moisture could reach up to -0.7 . Such a significant negative relationship also holds true on a daily basis over central Siberia in the past two decades. It is worth noting that air temperature and soil moisture in summer in the past two decades are anti-correlated virtually. In statistical terms, warm dry periods in summer coincide with the majority of wildfire occurrences (Extended Data Fig. 6) via boosting the readiness of vegetation and soil to burn. Fig. 2b clearly indicates that the summertime soil moisture has been descending with a rising air temperature since the beginning of 21st century. One exception is the anomalously hot summer in 2012 when soil was quite dry and the burned area in central Siberia peaked around 67,000 km². This exactly proves how important the warming climate might be in central Siberian wildfire. As the Arctic climate warms up, in 2019–

2021 when surface moisture was dried down to $\sim 345 \text{ kg m}^{-3}$, burned areas of central Siberian wildfire more than twice the 20-year average of $27,000 \text{ km}^2$, readily hitting the peak in climatically anomalous year 2012. The great importance of soil moisture in fostering wildfire activities and its close linkage with air temperature raise the question of how the warming climate impacts Siberian soil moisture and wildfires.

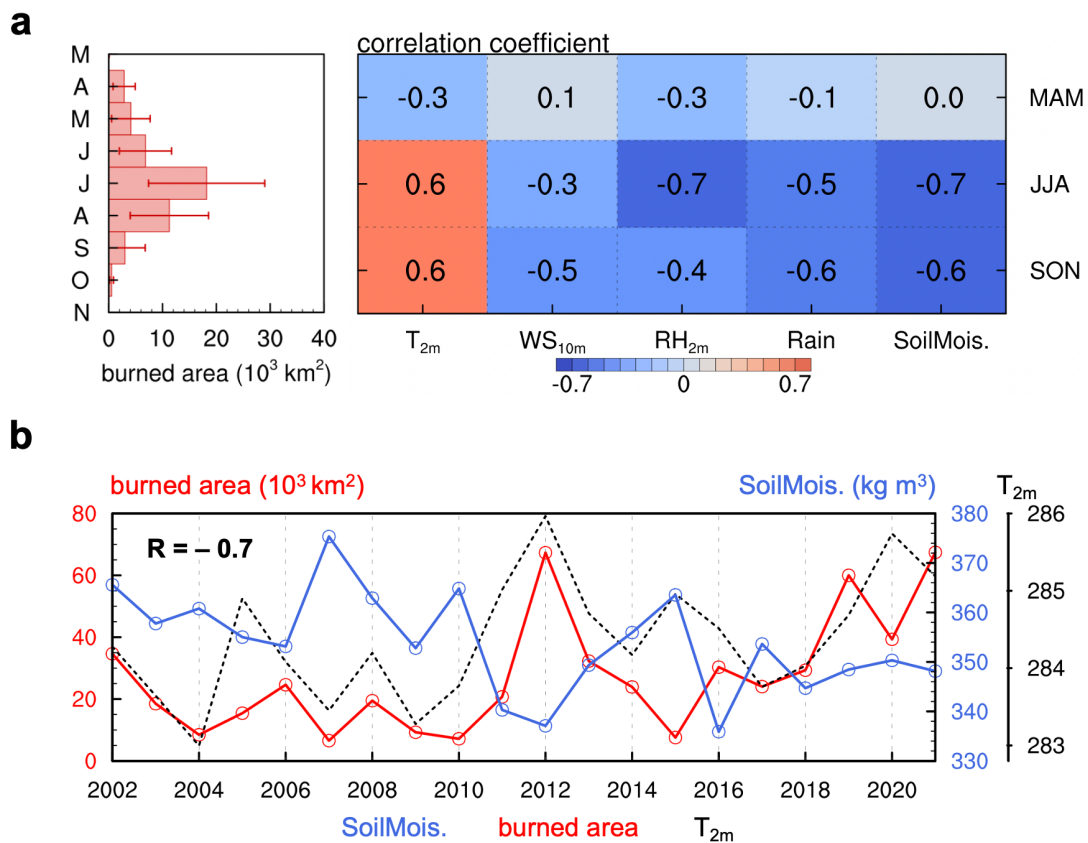


Fig 2. Relationship of wildfire and meteorology in central Siberia in different seasons. **a**, Seasonality of burned area of central Siberian wildfire averaged for 2002–2021 (left panel). Stand deviations are shown by whiskers. A correlation coefficient plot between seasonal wildfire burned areas in central Siberia (black rectangle in Fig. 1a) and various meteorological parameters in the past two decades (right panel), including 2-meter air temperature (T_{2m}), 10-meter wind speed (WS_{10m}), 2-meter relative humidity (RH_{2m}), rainfall rate (Rain), and surface soil moisture (SoilMois.). **b**, Interannual variability of central Siberian wildfire and soil moisture in summer during 2002–2021. The correlation coefficient of fire area and soil moisture is labeled in the top left corner.

By analyzing daily meteorological conditions from 20-year ERA5 reanalysis data, we found that such a prominent drop of soil moisture in central Siberia is closely related to a rapid Arctic warming. As the direct driver of soil water storage, precipitation has been receding over this region (Fig. 3), with a regional-average trend of -0.2 mm/year. There are two main causes for increasingly less precipitation and both are linked with Arctic warming. On one hand, the substantial warming of air temperature would certainly lead to a decrease in relative humidity, lowering precipitable water in the atmosphere (Fig. 3a and b). Over the Siberian Plateau where the air temperature warmed by approximately 0.08 K/year, the decrease in relative humidity could reach up to ~ 0.2 %/year. On the other hand, changes in large-scale circulation and storm tracks associated with Arctic warming also play a vital role in less precipitation in Siberia. It is well acknowledged that, over northern Eurasia, the establishment of the mid-summer precipitation belt is largely supported by the regional storm track activities, characterized by high-frequency transient eddies^{37,38}. The 20-year trend of mean standard deviation (SD) of 10-day high-pass filtered daily 500-hPa geopotential height and 300-hPa meridional wind, which is the indicator for the intensity of synoptic-scale eddy activity, exhibits clear declining signals at 55°N – 70°N (Extended Data Fig. 7). Accordingly, the transient eddy meridional moisture flux (see Method), which represents the moisture transport by synoptic-scale storms and largely contributes to the precipitation over Siberia³⁷, has been decreasing during the past two decades with a rate of over -0.5 g kg⁻¹/year in the Siberian Plateau (Fig. 3c). Such weakening summer storm tracks in Siberia are closely

linked with the warming Arctic, since that the reduced low-level baroclinicity associated with the decreasing poleward temperature gradients could diminish synoptic-scale cyclogenesis and then weaken the storm tracks^{39–41}. As a result, the strong reductions in summertime soil water availability induced by less precipitation could lead to higher fire danger in central Siberia.

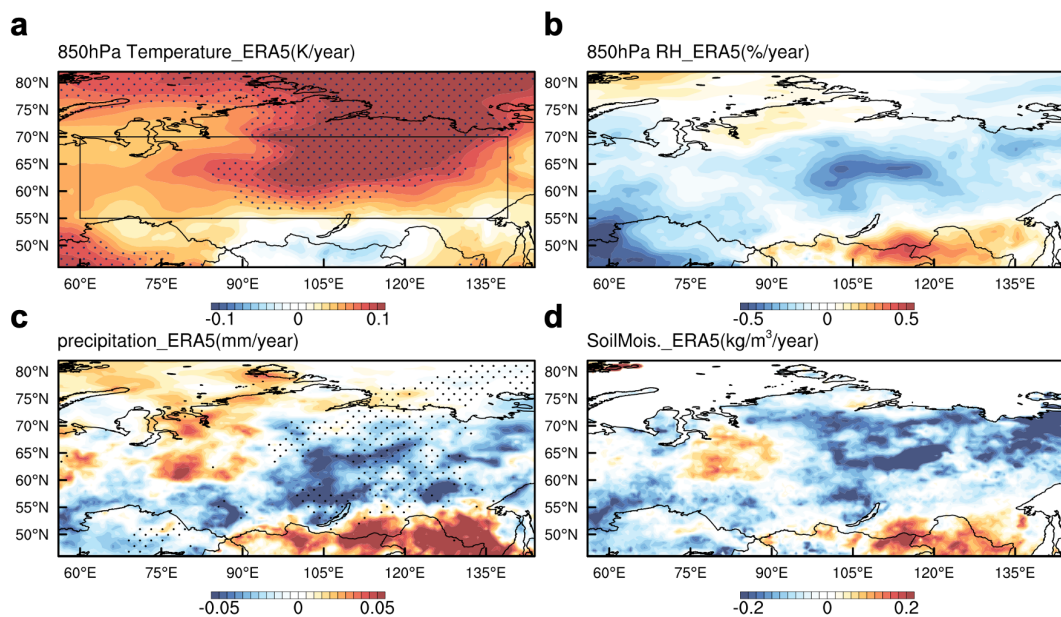


Fig 3. Arctic warming decreases summertime soil moisture in central Siberia. a, summertime 850-hPa air temperature trend derived from ERA5 reanalysis data during 2002–2021. Areas with a significant warming tendency ($p > 0.9$) are marked by black dots. **b,** summertime trend of relative humidity (RH) at 850 hPa. **c,** spatial distribution of trend in summertime precipitation. Black dots indicate areas with a decreasing trend greater than $-0.5 \text{ g kg}^{-1}/\text{year}$ in transient meridional moisture flux. **d,** soil moisture (SoilMois.) trend during the past two decades.

Smoke aerosols-cloud interaction amplifies the wildfires

The rising wildfire in central Siberia is expected to release an increasingly large quantity of smoke aerosols into the atmosphere. Another interesting phenomenon is that the cloud radius observed by MODIS show a declining tendency and anti-correlated with aerosol optical depth (AOD), with a correlation coefficient of 0.6 (Extended Data Fig. 8a). It is well proven that smoke aerosols can pose feedback to the climate system via directly perturbing radiation transfer (aerosol-radiation interaction) or indirectly serving as cloud condensation nuclei (CCN) and modifying the cloud microphysics properties (aerosol-cloud interactions)^{42,43}. In the central Siberia, such feedback between wildfire and regional climate might play a role in increasing wildfire activities. To quantitatively understand the role of smoke aerosols on climatic condition, we performed model simulations using the state-of-the-art climate-chemistry coupled model Community Earth System Model (CESM version 2.1.0, see Method). Multiple observational datasets were collected to validate the model performance of reproducing climate and pollution condition (Extended Data Figs. 9 and 10).

Unlike other biomass-burning regions, in Siberia where smoldering combustion of boreal forest and tundra consume a large proportion of biomass⁴⁴, carbonaceous aerosol emission is exceptionally pronounced (Extended Data Fig. 8b). The sensitivity simulations clearly show that emission-intensive Siberian wildfires give rise to summertime haze pollution over the high-northern-latitude region, with the smoke plume stretching

from 60°E to 150°E. Such a high aerosol-containing pollution belt is overlapped with thick low clouds (Extended Data Fig. 11a). In vertical, the summertime cloud base in this region is generally beneath 900 hPa, making itself easily to be mixed with fire smoke aerosols, which is clearly illustrated by both satellite observations and model simulations (Fig. 4a and Extended Data Fig. 11b). The model results show that the fire-emitted aerosols elevate the regional-averaged column CCN number at 0.1% water vapor supersaturation by 39.2% ($1.3 \times 10^7 \text{ \#/cm}^2$) over central Siberia.

The fire-induced bursting CCN is capable of acting as nuclei for water droplet formation and perturb the cloud microphysics⁴⁵. Over a pristine region like Siberia, the cloud formation could be very sensitive to the available aerosol in the atmosphere⁴⁶. According to sensitivity simulations, over central Siberia, more CCN availability from wildfires more than double the regional column-integrated cloud drop number concentration (CDNC) (Extended Data Fig. 12). Under a certain level of liquid water content in the atmosphere, more CDNC could certainly result smaller cloud droplet radius. Accordingly, the regional-mean droplet effective radius declines 0.4 μm over central Siberia, thereby inhibiting the precipitation and further lowering soil moisture (Fig. 4c, d). Quantitatively, smoke aerosols would induce a decline of almost 8% in summertime rainfall over central Siberia. Such a prominent precipitation suppression is due mainly to the CCN-limited cloud-aerosol regime and fire-smoke aerosol accumulation^{27,46}.

In consequence, less rainfall tends to facilitate rigorous and extended hydrological drought, further aggravating the flammability of soil and vegetation by lowering soil

moisture. It means that in addition to a warming and drying climate that is fueling wildfires, smoke aerosols emitted from wildfires could suppress the rainfall and further dry the soil, which might also play an important role in fire intensification in central Siberia. Wildfire intensification, smoke aerosols and its impact on cloud has been forming a self-amplifying feedback loop in central Siberia, making wildfire in this region extremely vulnerable to climate change. Such positive feedbacks underscore the fact that increasing wildfire activity is not just a consequence of climate change, but also an active participant.

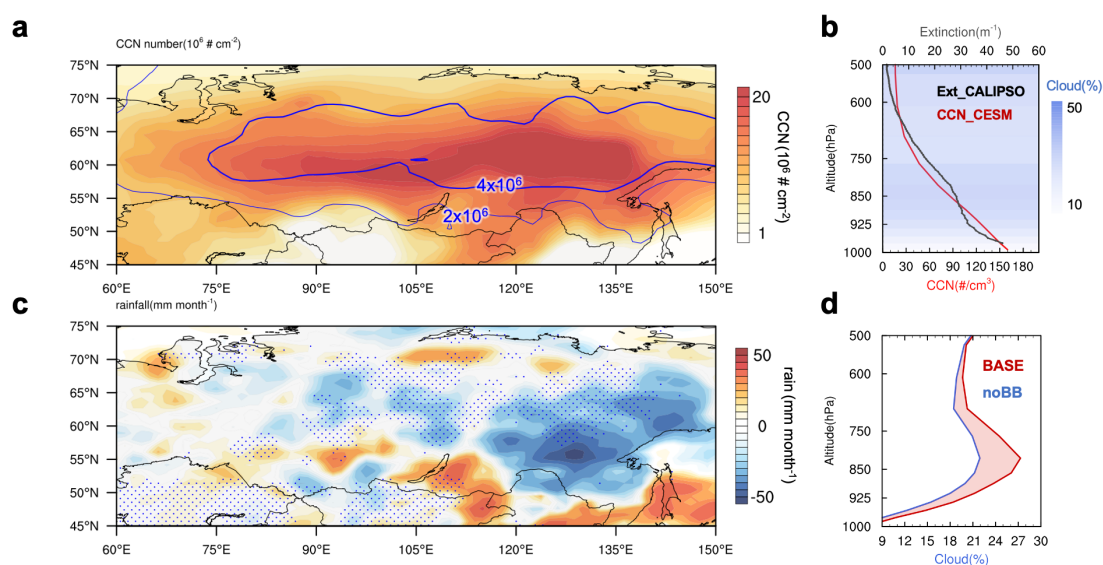


Fig 4. Impact of smoke aerosol-cloud interaction. **a**, Spatial distributions of summer-time column integrated cloud condensation nuclei (CCN) concentration (contour) and changes in column-integrated cloud droplet number due to wildfire smoke aerosols based on CESM climatology simulations (isolines, with the unit of # cm^{-2}). **b**, Vertical profile CALIPSO-observed aerosol extinction simulated (Ext_CALIPSO) and CESM-simulated CCN number concentration (CCN_CESM) over eastern Siberia. The vertical distribution of cloud fraction is shown in contour. **c**, Map showing changes in summertime rainfall (contour) and soil moisture (blue dots show regions with soil moisture decrease more than 10 kg/m^3) due to wildfire BB aerosols. **d**, Vertical profile of the increases in cloud

fraction based on parallel CESM simulations with (BASE run) and without wildfire emission (noBB run).

Discussions

Observational evidence and climatology modeling reveal that a warming Arctic and fire self-amplification due to smoke aerosol have been compounding the Siberian wildfire in the past two decades, and eastern Siberia is identified as a regional “hot spot” for fire poleward expansion and intensification. Given that Arctic warming is very likely to be further escalated in the future, here we apply 20 state-of-the-art global climate simulations under different shared socioeconomic pathways, namely SSP1–2.6 and SSP 2–4.5 from CMIP6 (Methods), to characterize the fire regime and its potential changes by mid- and late 21st century (Fig. 5). Arctic is projected to be further warmed by 4.7 ± 0.9 °C and 7.6 ± 1.1 °C around 2100, with the summer warming in eastern Siberia by 4.7 ± 0.1 °C and 4.8 ± 0.2 °C under SSP1–2.6 and SSP2–4.5 pathways, respectively.

The future warming could further reduce the soil water storage at high latitudes in the Arctic circumpolar region via fast evapotranspiration associated with higher vapor pressure deficit^{47,48}. Furthermore, a weaker and pole-ward-shifted jet stream under a warming Arctic may substantially increase the risk of concurrent extreme droughts and heat waves, potentially drying out the soil⁴⁹. As illustrated, the soil moisture in eastern Siberia at the end of this century is subject to a decline of ~28% and ~39% under SSP1–

2.6 and SSP2–4.5 pathways, respectively. On the basis of the correlation of fire intensity with soil moisture, the fire severity over this region is predicted to increase by 200–350% by the end of 21st century. Such fire intensification and poleward expansion might be even more pronounced since the increasing lightning frequency is expected to further compound the fire intensification in Siberia¹⁰. Even worse, under Arctic warming in the future, Siberian permafrost may increase fire frequency in what had traditionally been a low flammability landscape³⁹, presenting new challenges for fire management and climate adaptation in the pan-Arctic region.

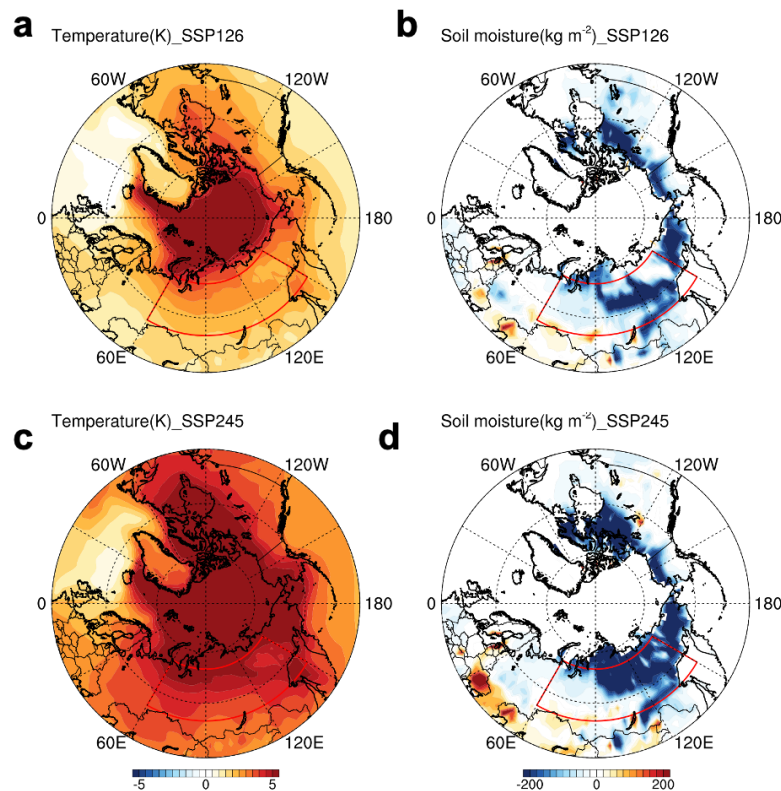


Fig 5. Future fire intensification under a warming Arctic. **a**, Near-surface air temperature increase from this decade (2015–2025) to the end of the century (2090–2100) under the SSP1–2.6 scenario based on ten CMIP6 experiments. **b**, Soil moisture changes by the end of the century under the SSP1–2.6 pathway. **c**, Same with **a** but under SSP2–4.5 pathway. **d**, Same with **b** but under SSP2–4.5 pathway.

Methods

Wildfire dataset and satellite observations

The Moderate Resolution Imaging Spectroradiometer (MODIS) onboard the Terra and Aqua satellites has been monitoring fires since the year 2001, and the thermal anomalies and fire product (MOD14A1 and MYD14A1) provides the location and timing for the fires globally. The Terra and Aqua combined MCD64A1 Burned Area data product is a monthly, global gridded 500-meter product containing per-pixel burned-area and quality information. The MCD64A1 burned-area mapping approach employs MODIS Surface Reflectance imagery coupled with 1 kilometer (km) MODIS active fire observations⁵⁰. Since observations from both MODIS instruments aboard the Terra and Aqua satellites are applied, the possibility of “double-counting” the same fire on a single day occurs. To avoid double-counting, we used burned-area derived by The Fire Inventory from NCAR (FINN version 1.5), which removes fire detections that fall within a 1 km² radius of another fire detection on daily basis. Therefore, for each 1 km² hot spot, there can be only one fire per day⁵⁰. FINN model provides daily high-resolution burned area and emissions of open burning at a horizontal resolution of 1 km × 1km. The burned area data during the time period from 2002 to 2021 is adopted in this study. To validate the performance of FINN burned area used in this work, we also include the Global Fire Emissions Database (GFED) data for comparisons, which combines satellite information on fire activity and vegetation productivity to estimate gridded monthly burned

area and fire emissions⁵⁰. We compare the fire detection from different products/datasets, including MCD64A1 burned area, FINN burned area and Global Fire Emissions Database (GFED) carbon emission dataset. As shown in Extended Data Fig. 3, all the dataset shows a similar interannual variability in wildfires in eastern Siberia.

To demonstrate the horizontal and vertical structure of aerosol and cloud, MODIS monthly aerosol optical depth and cloud fraction retrievals (MOD08 and MOD06) during 2002 to 2021 and Cloud-Aerosol Lidar and Infrared Pathfinder Satellite Observations (CALIPSO, level 3 aerosol profile product) that provides information on vertical distributions of smoke extinction and cloud since 2007 are also employed. Permafrost extent in the Northern Hemisphere with the spatial resolution around 1km is obtained from Permafrost data products from the European Space Agency's Climate Change Initiative Permafrost project (ESACCI, version 3.0) for the period 1997–2019³³.

Atmospheric reanalysis data

Historical meteorologic parameters since the year 2002 are acquired from the fifth generation of European Centre for Medium-Range Weather Forecasts (ECMWF) ERA5 reanalysis data. ERA5 reanalysis data provides hourly estimates of a large number of atmospheric, land and oceanic climate variables, which are produced using data assimilation and model forecasts of the ECMWF Integrated Forecast System (IFS), with a horizontal resolution of $0.25^{\circ} \times 0.25^{\circ}$ and 137 hybrid levels from the surface up to a

height of approximately 80 km. Here, hourly data of 2-meter air temperature, 2-meter relative humidity, evapotranspiration from the surface, 10-meter wind speed, soil water content at the surface, wind and cloud at different pressure levels, and precipitation during the time period from 2000 to 2021 are utilized to investigate the climate changes in the pan-Arctic region.

Calculation of transient moisture flux

The transient moisture flux is used to represent the moisture transport by synoptic-scale eddies, as it largely contributes to the precipitation over eastern Siberia³⁷. The total moisture flux (monthly mean of hourly flux) could be separated as the stationary component (derived directly from the monthly fields) and the transient component. Thus, the transient term is obtained by subtracting the stationary component from the total flux in this work. Particularly, we consider the vertically integrated from 1000 hPa to 500 hPa of the poleward transient moisture flux ($\text{g m}^{-1} \text{s}^{-1}$) as Eq. 1, since it dominates the total moisture flux convergence in the Arctic region⁵¹.

$$F_{transient} = -\frac{1}{g} \int_{p_0}^{p_t} (\overline{q'v'}) dp = -\frac{1}{g} \int_{p_0}^{p_t} (\overline{qv} - \bar{q}\bar{v}) dp,$$

Where the overbars represent the time averages, and the primes represent the transient term. p_0 and p_t are 1000 hPa and 500 hPa, respectively. Besides, the 850-hPa transient moisture flux ($(\overline{q'v'})_{850}$, $\text{m s}^{-1} \text{g kg}^{-1}$) is also used to depict the synoptic-scale eddy activities transporting water vapor poleward at the lower troposphere.

Future climate projection

Projections of climate change help estimate the future wildfire severity in Siberia. Phase 6 of the Coupled Model Intercomparison Project (CMIP6)⁵², which has developed well-defined climate model experiment protocols, formats, and standards, plays a fundamental role in improving understanding of the climate change as well as characterizing risks in the future. Multi-model climate projected air temperature and soil moisture by the end of this century within CMIP6 are collected. Monthly air temperature and soil moisture projections from 20 simulations by global climate models, including UKESM1-0-LL, BCC-CSM2-MR, MIROC6, FGOALS-f3-L and CESM2 under SSP1–2.6 and SSP2–4.5 scenarios are used as the ensemble of the future conditions.

CESM simulations

To investigate the climate feedback of fire smoke aerosol, we conducted sensitivity simulations using the Community Atmosphere Model Version 6 (CAM6) with chemistry of the National Center for Atmospheric Research (NCAR) Community Earth System Model (CESM version 2.1.0)⁵³. New chemical and physical representations of direct and indirect aerosol effects and their interactions with clouds are among the improvements made by the CAM6. Meanwhile, a default of the Modal Aerosol Model

version 4 (MAM4) with improved treatment of aerosols has been implemented⁵⁴. Additional updates include the Morrison-Gottelman cloud microphysics scheme, aerosol-temperature-dependent mixed-phase ice nucleation, a unified turbulence scheme for different cloud types, etc. The CESM2 has been identified as one of the most skillful models that could well represent the present climate status³⁷. In this study, two parallel simulations, BASE run and noBB run, have been performed at $0.9^\circ \times 1.25^\circ$ horizontal grids with 32 vertical levels. Both tests run for 10 years to gain a balanced climatology after a 1-year spin-up. All emission inventories implemented are from the dataset representing the climatological status in the 2010s developed for assessments in the CMIP6^{55,56}, and have been re-gridded to the model grids. The two simulations share exactly the same model configuration and anthropogenic inventories, while only differ from each other in biomass burning emissions. The BASE run used the historical global biomass burning emissions for CMIP6⁵⁶, averaging between 2006 and 2014 and cycling for every model year, whereas the noBB run excluded the biomass burning emissions. The difference between the outputs of the two simulations has then been regarded as the response to the wildfire emissions.

Reference

1. Pan, Y. *et al.* A large and persistent carbon sink in the world's forests. *Science* **333**, 988–993 (2011).
2. Schuur, E. A. G. *et al.* Climate change and the permafrost carbon feedback. *Nature* **520**, 171–179 (2015).
3. Miner, K. R. *et al.* Permafrost carbon emissions in a changing Arctic. *Nat. Rev. Earth Environ.* **3**, 55–67 (2022).
4. Hugelius, G. *et al.* Estimated stocks of circumpolar permafrost carbon with quantified uncertainty ranges and identified data gaps. *Biogeosciences* **11**, 6573–6593 (2014).
5. Bond-Lamberty, B., Peckham, S. D., Ahl, D. E. & Gower, S. T. Fire as the dominant driver of central Canadian boreal forest carbon balance. *Nature* **450**, 89–92 (2007).
6. Turetsky, M. R. *et al.* Recent acceleration of biomass burning and carbon losses in Alaskan forests and peatlands. *Nat. Geosci.* **4**, 27–31 (2011).
7. Walker, X. J. *et al.* Increasing wildfires threaten historic carbon sink of boreal forest soils. *Nature* **572**, 520–523 (2019).
8. Zheng, B. *et al.* Increasing forest fire emissions despite the decline in global burned area. *Sci. Adv.* **7**, (2021).

9. Huang, J. *et al.* Recently amplified arctic warming has contributed to a continual global warming trend. *Nat. Clim. Chang.* **7**, 875–879 (2017).
10. Chen, Y. *et al.* Future increases in Arctic lightning and fire risk for permafrost carbon. *Nat. Clim. Chang.* **11**, 404–410 (2021).
11. Francis, J. A., Vavrus, S. J. & Cohen, J. Amplified Arctic warming and mid-latitude weather: new perspectives on emerging connections. *Wiley Interdiscip. Rev. Clim. Chang.* **8**, (2017).
12. Post, E. *et al.* The polar regions in a 2°C warmer world. *Sci. Adv.* **5**, (2019).
13. Abatzoglou, J. T., Rupp, D. E., O’Neill, L. W. & Sadegh, M. Compound Extremes Drive the Western Oregon Wildfires of September 2020. *Geophys. Res. Lett.* **48**, (2021).
14. Bessie, W. C. & Johnson, E. A. The relative importance of fuels and weather on fire behavior in subalpine forests. *Ecology* **76**, 747–762 (1995).
15. Westerling, A. L., Hidalgo, H. G., Cayan, D. R. & Swetnam, T. W. Warming and earlier spring increase Western U.S. forest wildfire activity. *Science* **313**, 940–943 (2006).
16. Liu, Y., Stanturf, J. & Goodrick, S. Trends in global wildfire potential in a changing climate. *For. Ecol. Manage.* **259**, 685–697 (2010).
17. McCarty, J. L., Smith, T. E. L. & Turetsky, M. R. Arctic fires re-emerging. *Nat. Geosci.* **13**, 658–660 (2020).

18. Rein, G. & Huang, X. Smouldering wildfires in peatlands, forests and the arctic: Challenges and perspectives. *Curr. Opin. Environ. Sci. Heal.* **24**, 100296 (2021).
19. Mccarty, J. L. *et al.* Reviews and syntheses: Arctic fire regimes and emissions in the 21st century. *Biogeosciences* **18**, 5053–5083 (2021).
20. Talucci, A. C., Loranty, M. M. & Alexander, H. D. Siberian taiga and tundra fire regimes from 2001-2020. *Environ. Res. Lett.* **17**, 025001 (2022).
21. Lin, S., Liu, Y. & Huang, X. Climate-induced Arctic-boreal peatland fire and carbon loss in the 21st century. *Sci. Total Environ.* **796**, 148924 (2021).
22. Tomshin, O. & Solovyev, V. Spatio-temporal patterns of wildfires in Siberia during 2001–2020. *Geocarto Int.* (2021) doi:10.1080/10106049.2021.1973581.
23. Irannezhad, M., Liu, J., Ahmadi, B. & Chen, D. The dangers of Arctic zombie wildfires. *Science* **369**, 1171 (2020).
24. Giglio, L., Randerson, J. T. & Van Der Werf, G. R. Analysis of daily, monthly, and annual burned area using the fourth-generation global fire emissions database (GFED4). *J. Geophys. Res. Biogeosciences* **118**, 317–328 (2013).
25. Lu, Z. *et al.* Biomass smoke from southern Africa can significantly enhance the brightness of stratocumulus over the southeastern Atlantic Ocean. *Proc. Natl. Acad. Sci. U. S. A.* **115**, 2924–2929 (2018).

26. Kochanski, A. K. *et al.* Modeling Wildfire Smoke Feedback Mechanisms Using a Coupled Fire-Atmosphere Model With a Radiatively Active Aerosol Scheme. *J. Geophys. Res. Atmos.* **124**, 9099–9116 (2019).
27. Petäjä, T. *et al.* Influence of biogenic emissions from boreal forests on aerosol–cloud interactions. *Nat. Geosci.* **15**, 42–47 (2022).
28. Aubry-Wake, C., Bertoincini, A. & Pomeroy, J. W. Fire and Ice: The Impact of Wildfire-Affected Albedo and Irradiance on Glacier Melt. *Earth's Futur.* **10**, e2022EF002685 (2022).
29. Piao, J., Chen, W., Chen, S., Gong, H. & Zhang, Q. Summer water vapor Sources in Northeast Asia and East Siberia revealed by a moisture-tracing atmospheric model. *J. Clim.* **33**, 3883–3899 (2020).
30. Kirillina, K., Shvetsov, E. G., Protopopova, V. V., Thiesmeyer, L. & Yan, W. Consideration of anthropogenic factors in boreal forest fire regime changes during rapid socio-economic development: case study of forestry districts with increasing burnt area in the Sakha Republic, Russia. *Environ. Res. Lett.* **15**, 035009 (2020).
31. Rein, G. Smouldering Fires and Natural Fuels. *Fire Phenom. Earth Syst. An Interdiscip. Guid. to Fire Sci.* 15–33 (2013) doi:10.1002/9781118529539.ch2.

32. Masrur, A., Petrov, A. N. & DeGroot, J. Circumpolar spatio-temporal patterns and contributing climatic factors of wildfire activity in the Arctic tundra from 2001-2015. *Environ. Res. Lett.* **13**, 14019 (2018).
33. Obu, J. *et al.* ESA Permafrost Climate Change Initiative (Permafrost_cci): Permafrost extent for the Northern Hemisphere, v3.0. *NERC EDS Centre for Environmental Data Analysis*
<https://catalogue.ceda.ac.uk/uuid/6e2091cb0c8b4106921b63cd5357c97c>
(2021).
34. Xing, C. *et al.* Observations of the vertical distributions of summertime atmospheric pollutants and the corresponding ozone production in Shanghai, China. *Atmos. Chem. Phys.* **17**, 14275–14289 (2017).
35. Smith, A. J. P., Smith, D. M., Cohen, J. & Jones, M. W. Arctic warming amplifies climate change and its impacts. *Sci. Rev.* (2021)
[doi:10.5281/ZENODO.5596791](https://doi.org/10.5281/ZENODO.5596791).
36. Bartsch, A., Balzter, H. & George, C. The influence of regional surface soil moisture anomalies on forest fires in Siberia observed from satellites. *Environ. Res. Lett.* **4**, 045021 (2009).
37. Fukutomi, Y., Masuda, K. & Yasunari, T. Role of storm track activity in the interannual seesaw of summer precipitation over northern Eurasia. *J. Geophys. Res. Atmos.* **109**, 2109 (2004).

38. Serreze, M. C. *et al.* Large-scale hydro-climatology of the terrestrial Arctic drainage system. *J. Geophys. Res. D Atmos.* **108**, ALT 1-1 (2003).
39. Nitzbon, J. *et al.* Fast response of cold ice-rich permafrost in northeast Siberia to a warming climate. *Nat. Commun.* **11**, 2201 (2020).
40. Hoskins, B. & Woollings, T. Persistent Extratropical Regimes and Climate Extremes. *Curr. Clim. Chang. Reports* **1**, 115–124 (2015).
41. Coumou, D., Lehmann, J. & Beckmann, J. The weakening summer circulation in the Northern Hemisphere mid-latitudes. *Science* **348**, 324–327 (2015).
42. Gao, M., Ji, D., Liang, F. & Liu, Y. Attribution of aerosol direct radiative forcing in China and India to emitting sectors. *Atmos. Environ.* **190**, 35–42 (2018).
43. Schill, G. P. *et al.* Widespread biomass burning smoke throughout the remote troposphere. *Nat. Geosci.* **13**, 422–427 (2020).
44. Hu, Y., Fernandez-Anez, N., Smith, T. E. L. & Rein, G. Review of emissions from smouldering peat fires and their contribution to regional haze episodes. *Int. J. Wildl. Fire* **27**, 293–312 (2018).
45. Rosenfeld, D. *et al.* Global observations of aerosol-cloud-precipitation-climate interactions. *Rev. Geophys.* **52**, 750–808 (2014).
46. Mauritsen, T. *et al.* An Arctic CCN-limited cloud-aerosol regime. *Atmos. Chem. Phys.* **11**, 165–173 (2011).

47. Zhang, Y. *et al.* Evaporation Processes and Changes Over the Northern Regions. *Arct. Hydrol. Permafr. Ecosyst.* 101–131 (2021) doi:10.1007/978-3-030-50930-9_4.
48. Dai, A., Zhao, T. & Chen, J. Climate Change and Drought: a Precipitation and Evaporation Perspective. *Curr. Clim. Chang. Reports* **4**, 301–312 (2018).
49. Zscheischler, J. & Seneviratne, S. I. Dependence of drivers affects risks associated with compound events. *Sci. Adv.* **3**, (2017).
50. Wiedinmyer, C. *et al.* The Fire INventory from NCAR (FINN): a high resolution global model to estimate the emissions from open burning. *Geosci. Model Dev* **4**, 625–641 (2011).
51. Oshima, K., Yamazaki, K., Oshima, K. & Yamazaki, K. Difference in seasonal variation of net precipitation between the Arctic and Antarctic regions. *GeoRL* **33**, L18501 (2006).
52. Eyring, V. *et al.* Overview of the Coupled Model Intercomparison Project Phase 6 (CMIP6) experimental design and organization. *Geosci. Model Dev.* **9**, 1937–1958 (2016).
53. Danabasoglu, G. *et al.* The Community Earth System Model Version 2 (CESM2). *J. Adv. Model. Earth Syst.* **12**, e2019MS001916 (2020).

54. Liu, X. *et al.* Description and evaluation of a new four-mode version of the Modal Aerosol Module (MAM4) within version 5.3 of the Community Atmosphere Model. *Geosci. Model Dev.* **9**, 505–522 (2016).
55. Hoesly, R. M. *et al.* Historical (1750-2014) anthropogenic emissions of reactive gases and aerosols from the Community Emissions Data System (CEDS). *Geosci. Model Dev.* **11**, 369–408 (2018).
56. Van Marle, M. J. E. *et al.* Historic global biomass burning emissions for CMIP6 (BB4CMIP) based on merging satellite observations with proxies and fire models (1750-2015). *Geosci. Model Dev.* **10**, 3329–3357 (2017).

Code availability

The code of the CESM2 model used in this study is available from

https://www.cesm.ucar.edu/models/cesm2/release_download.html.